Measurement of amide proton exchange rates and NOEs with water in $^{13}C/^{15}N$-enriched calcineurin B

Stephan Grzesiek and Ad Bax

*Laboratory of Chemical Physics, National Institute of Diabetes and Digestive and Kidney Diseases,
National Institutes of Health, Bethesda, MD 20892, U.S.A.*

SUMMARY

A rapid and sensitive 2D approach is presented for measuring amide proton exchange rates and the NOE interaction between amide protons and water. The approach is applicable to uniformly $^{13}C/^{15}N$-enriched proteins and can measure magnetization exchange rates in the 0.02 to > 20 s^{-1} range. The experiments rely on selective excitation of the water resonance, coupled with purging of underlying H$^\alpha$ resonances, followed by NOESY- or ROESY-type transfer to amide protons, which are dispersed by the amide ^{15}N frequencies in an HSQC-type experiment. Two separate but interleaved experiments, with and without selective inversion of the H$_2$O resonance, yield quantitative results. The method is demonstrated for a sample of the calcium-binding protein calcineurin B. Results indicate rapid amide exchange for the five calcineurin B residues that are analogous to the five rapidly exchanging residues in the 'central helix' of the homologous protein calmodulin.

INTRODUCTION

In proteins, magnetization can exchange between backbone amide protons and the aqueous solvent in two fundamentally different ways: chemical exchange and NOE-mediated magnetization transfer. The exchange rates of backbone amide protons with water are commonly interpreted in terms of hydrogen-bond stability and solvent accessibility (Englander and Kallenbach, 1984; Tüchsen and Woodward, 1985), whereas direct NOE interactions between amide protons and H$_2$O provide valuable distance information. These two types of magnetization exchange can be differentiated by comparing the results of NOESY and ROESY experiments (Otting and Wüthrich, 1989). Detailed studies of NOE interactions between the aqueous solvent and proteins (Clore et al., 1990; Otting et al., 1991a,b,c; Liepinsh et al., 1993; Xu et al., 1993), DNA (Kubinec and Wemmer, 1992; Liepinsh et al., 1992), and protein–DNA complexes (Qian et al., 1993) have provided valuable insights into the interaction between solvent and macromolecules. Usually, such studies require the recording of 3D datasets which sometimes have to be repeated at various

temperatures to differentiate intramolecular NOEs from intermolecular interactions on the basis of the temperature dependence of the water resonance. Here we demonstrate the use of simple and sensitive 2D analogs of these 3D experiments which are applicable to uniformly $^{13}C/^{15}N$-enriched macromolecules. They are based on selective excitation of the H_2O resonance and purging of the signals from ^{13}C-attached protons which accidentally overlap with the H_2O resonance. Alternatively, the long spin-locked relaxation time, $T_{1\rho}$, of the H_2O resonance can be used to selectively observe interactions with H_2O in macromolecules that are not isotopically enriched.

Pulse schemes

The pulse schemes for the NOESY and ROESY versions of the experiment are shown in Fig. 1. The first part of the pulse sequence (up to time point c) selectively inverts the H_2O resonance. Signals from ^{13}C-attached protons are eliminated by the 90° ^{13}C purge pulse applied at time b (Kogler et al., 1983; Ikura and Bax, 1992). In more detail, the first $90^{\circ}_{\phi 1}$ ^1H pulse (time a) is applied at low power (total duration 2 ms) with the ^1H carrier at the water frequency. Heteronuclear $^1J_{C\alpha H\alpha}$ dephasing of H^α magnetization, also excited by the selective pulse, is active for approximately half the duration of this shaped pulse. After a subsequent additional dephasing period δ of 2.4 ms, H^α_y magnetization has become antiphase with respect to its attached $^{13}C^\alpha$ spin $(2H^\alpha_x C^\alpha_z)$ and a carbon 90° purge pulse, applied at time b, converts the antiphase magnetization into unobservable 2-spin coherence $(-2H^\alpha_x C^\alpha_y)$. Next, the water magnetization is subjected to a low-power 180°_y refocusing pulse and after a second interval δ it is flipped parallel ($\phi_1 = -x$) or antiparallel ($\phi_1 = x$) to the z-axis by the 90°_x pulse. The two gradients G_1 are used to select for the 180° character of the 180°_y pulse (Bax and Pochapsky, 1992). Gradient G_2, applied at the beginning of the NOE mixing period τ, serves to dephase any residual transverse magnetization (Jeener et al., 1979), thereby also eliminating radiation damping effects. As a result, at time c the water magnetization points either along the +z ($\phi_1 = -x$) or -z ($\phi_1 = x$) axis with the magnetization of all other ^1H resonances largely aligned along +z, independent of ϕ_1. During the NOESY (Fig. 1A) or ROESY (Fig. 1B) mixing period, magnetization is transferred from the H_2O resonance to the amide protons which then are dispersed by the frequencies of their attached ^{15}N nuclei in a subsequent HSQC experiment (Bodenhausen and Ruben, 1980). One new element has been included in this HSQC experiment: a selective $90^{\circ}_{\phi 3}$ pulse (time d), applied to the water resonance immediately after the creation of $H^N_z N_z$ antiphase magnetization and followed by a pulsed field gradient (G_3), ensures that the water magnetization is along the -z axis during the first half of the t_1 evolution period. The water magnetization is then flipped back to the +z axis by the 180° (^1H) pulse applied at the center of t_1. The remainder of the pulse scheme is designed to leave the water magnetization along the +z axis. To this extent, the first 90° ^1H pulse of the final reverse INEPT transfer (time e) is preceded by a selective 90° pulse of opposite phase. Similarly, the final nonselective $180^{\circ}_{\phi 7}$ ^1H pulse is of opposite phase relative to its surrounding $90^{\circ}_{\phi 6}$ pulses. Together with the pulsed field gradients G_5, the $90^{\circ}_{\phi 6}$-$180^{\circ}_{\phi 7}$-$90^{\circ}_{\phi 6}$ pulse combination also provides a very high degree of water suppression (Piotto et al., 1992). The above described water flip-back procedure ensures that the slowly relaxing water magnetization, which serves as the source of the observed signal, resides along the +z axis for most of the measurement. Hence, even though the experiment is repeated at a rate that is more than twice the longitudinal relaxation rate of H_2O, the water resonance is not strongly attenuated. This type of flip-back operation is fully analogous to the flip-back procedure commonly used in solid-state heteronuclear cross-polarization experiments
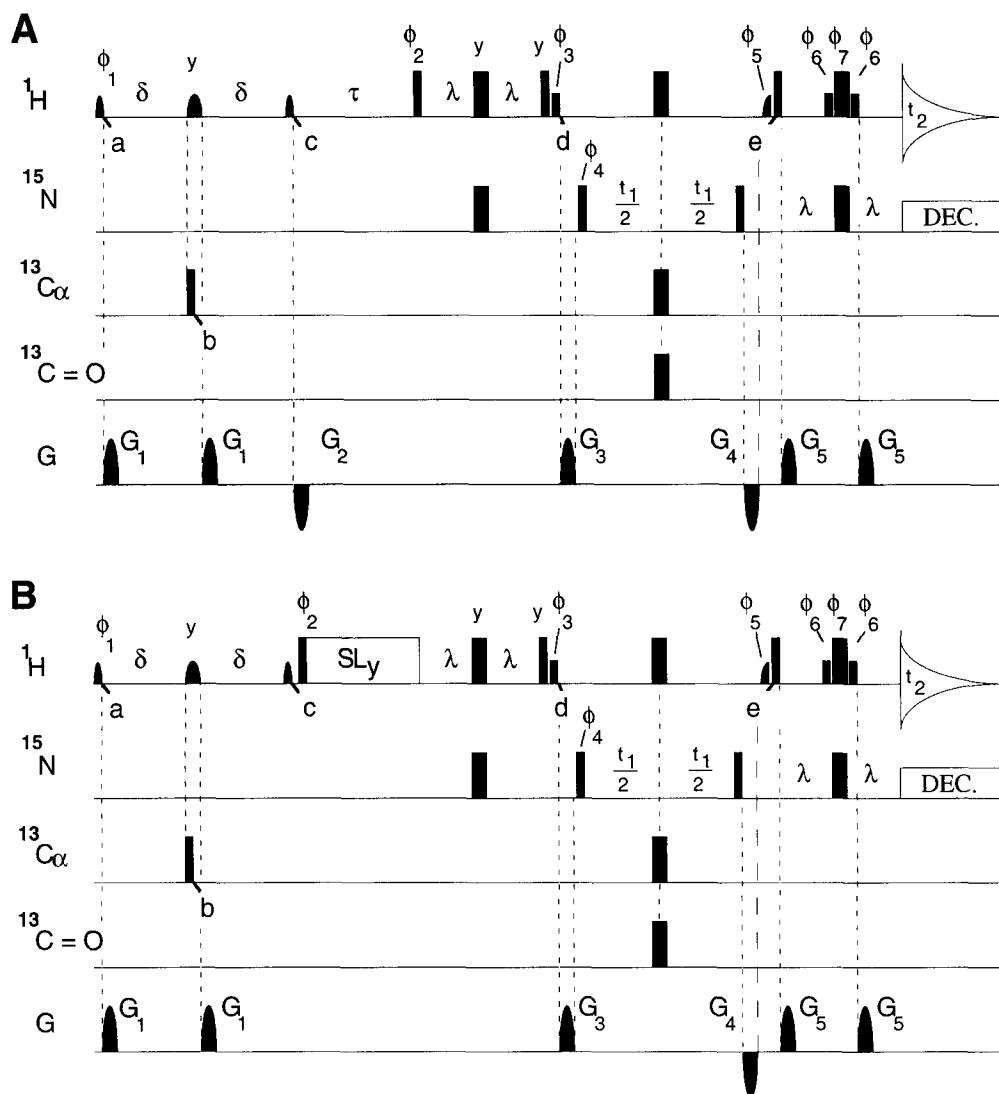
Fig. 1. Pulse scheme of the water-NOE (A) and water-ROE (B) experiments. Narrow and wide pulses correspond to 90° and 180° flip angles, respectively. Pulses for which the phase is not indicated are applied along the x-axis. The ^{1}H carrier frequency is set to the H_2O frequency, the ^{15}N, $^{13}C^\alpha$ and ^{13}CO carrier frequencies are set to 116.5, 56 and 177 ppm, respectively. ^{15}N decoupling is accomplished using WALTZ-16 modulation with a 1.5 kHz RF field. The first three (90°, 180°, 90°) ^{1}H pulses each have the shape of the center lobe of a (sin x)/x function and a duration of 2 ms for the 90° pulses. The $90°_{\phi 5}$ ^{1}H pulse has the profile of the left half of a Gaussian function and a width at half height of 500 μs. All other ^{1}H pulses are rectangular in shape. Their RF field strength is 270 Hz for the $90°_{\phi 3}$ and $90°_{\phi 6}$ pulses and 27 kHz for all other ^{1}H pulses. The 90° $^{13}C^\alpha$ pulse is applied at high power ($\gamma B_1/2\pi = 15$ kHz); the 180° $^{13}C^\alpha$ and ^{13}C=O decoupling pulses are applied at reduced power ($\gamma B_1/2\pi = 4.7$ kHz). Pulsed field gradients have a sine-bell amplitude profile with a strength of 25 G/cm at their center. Their durations are $G_{1,2,3,4,5} = 0.5$, 10.0, 2.5, 1.0, 0.4 ms. Delay durations are $\delta = 2.4$ ms, $\tau = 60$ ms, $\lambda = 2.25$ ms. Phase cycling of scheme (A) is as follows: $\phi_1 = x$; $\phi_2 = 4(x)$, $4(-x)$; $\phi_3 = 4(-x),4(x)$; $\phi_4 = x,-x$; $\phi_5 = -x$; $\phi_6 = 2(-x),2(x)$; $\phi_7 = 2(x),2(-x)$. Acq. = $2(x,-x),2(-x,x)$. Quadrature in the t_1 domain is obtained by changing the phase ϕ_4 in the usual States–TPPI manner (Marion et al., 1989). For the difference experiment, two sets of data are recorded in an interleaved manner with phases ϕ_1 and ϕ_3 either set to the values above, or inverted by 180°. For scheme (B) all parameters are the same as for (A). The additional spin-lock pulse along the y-axis, SL_y, has an RF field strength of 10 kHz and a duration of 25 ms.

(Tegenfeldt and Haeberlen, 1979; Ernst et al., 1987), and its use can benefit many of the modern heteronuclear NMR experiments (Grzesiek and Bax, 1993).

Magnetization transfer analysis

A quantitative description of the exchange with water for the amide proton magnetization M during the mixing period is easily derived from

$$dM_z/dt = -\rho_1(M_z - M_z^o) - k_N(M_z - M_z^{water})$$ (1a)

for the NOESY case and

$$dM_y/dt = -\rho_2 M_y - k_R(M_y - M_y^{water})$$ (1b)

for the ROESY case, where ρ_1 represents the amide proton-spin flip rate, ρ_2 equals $1/T_{1\rho}$, M_z^o is the amide proton z-magnetization at thermal equilibrium and M^{water} is the magnetization of the water at the start of the mixing period. The factors k_N and k_R are the pseudo-first-order rate constants for magnetization exchange between amide protons and H_2O during the NOESY and ROESY mixing periods, respectively. If magnetization exchange is due exclusively to hydrogen exchange, k_N equals k_R. At the other extreme, where hydrogen exchange is zero and all magnetization transfer is due to the NOE interaction, k_R approaches $-2k_N$ in the macromolecular limit. Values measured for ρ_1 and ρ_2 of the backbone amide protons in the rigid regions of calcineurin B are ca. 15 and 75 s^{-1}, respectively. Considering both the large molar excess of H_2O over the concentration of protein protons and the much longer T_1 and $T_{1\rho}$ values ($\sim$ 5 s) of H_2O, i.e., small ρ_1 and ρ_2 values, M_z^{water} and M_y^{water} in Eq. 1 may be considered constant during the mixing period. Under this assumption, the general solution to Eq. 1 is given by

$$M_z(t) = [M_z(0) - M_z(\infty)] \exp [-(\rho_1 + k_N)t] + M_z(\infty)$$ (2a)

$$M_y(t) = [M_y(0) - M_y(\infty)] \exp [-(\rho_2 + k_R)t] + M_y(\infty)$$ (2b)

where $M_z(\infty)$ and $M_y(\infty)$ are given by

$$M_z(\infty) = \frac{\rho_1 + k_N f}{\rho_1 + k_N} M_z^o$$ (3a)

$$M_y(\infty) = \frac{k_R f}{\rho_2 + k_R} M_z^o$$ (3b)

In these expressions f represents the fraction of the thermal equilibrium water magnetization which ends up parallel or antiparallel to the amide proton magnetization at the beginning of the mixing period. For a 2.1-s delay between scans, this value was measured to be f^+ = 0.73 (parallel) and f^- = −0.74 (antiparallel). These relatively low values result from a 9% loss during the first three water inversion pulses and an 8% loss during the rest of the pulse sequence due to relaxation and pulse imperfections. Therefore the water z-magnetization at the beginning of the acquisition period is only $\sim$ 67% of its equilibrium value. During the 2.1-s relaxation delay between scans this fraction increases to $\sim$ 80%.

The protein z-magnetization is zero at the start of data acquisition and recovers exponentially with longitudinal relaxation rate $\rho_{1,P} = (1.4 \text{ s})^{-1}$, resulting also in a value at the start of the pulse sequence that is ~ 80% of its thermal equilibrium value after a 2.1-s recovery delay. Water and protein magnetization therefore are in equilibrium with each other at the start of the pulse sequence, and to a good approximation both $M_z(0)$ and $M_y(0)$ in Eq. 2 are equal to 0.8 M_z^o.

Equation 3, which applies to the cases where the water magnetization is parallel (f^+) or antiparallel (f^-) to the amide proton magnetization, can now be substituted into Eq. 2 and the time course of the amide proton magnetization during the mixing periods, $M^+(t)$ and $M^-(t)$, respectively, can be calculated. Taking the difference between $M^+(t)$ and $M^-(t)$ and normalizing the result by the sum of $M^+(t)$ and $M^-(t)$ one arrives at the following equations:

$$\zeta_{NOE}(t) = \frac{M_z^+ (t) - M_z^- (t)}{M_z^+ (t) + M_z^- (t)}$$

$$= \frac{k_N(f^+ - f^-)[1 - \exp(-(\rho_1 + k_N)t)] \, M_z^o}{[2\rho_1 + k_N(f^+ + f^-)][1 - \exp(-(\rho_1 + k_N)t)] \, M_z^o + 2(\rho_1 + k_N) \exp(-(\rho_1 + k_N)t) \, M_z(0)} \tag{4a}$$

for the NOESY and

$$\zeta_{ROE}(t) = \frac{M_y^+ (t) - M_y^- (t)}{M_y^+ (t) + M_y^- (t)}$$

$$= \frac{k_R(f^+ - f^-)[1 - \exp(-(\rho_2 + k_R)t)] \, M_y^o}{k_R(f^+ + f^-)[1 - \exp(-(\rho_2 + k_R)t)] \, M_y^o + 2(\rho_2 + k_R) \exp(-(\rho_2 + k_R)t) \, M_y(0)} \tag{4b}$$

for the ROESY mixing period.

The rates $(\rho_1 + k_N)$ and $(\rho_2 + k_R)$ are determined from separate relaxation experiments (see below). Equation 5 is then easily inverted to yield the rates k_N and k_R from the measured values of ζ_{NOE} and ζ_{ROE}:

$$k_N = \frac{2\zeta_{NOE}(\rho_1 + k_N) \{M_z(0) + [\exp((\rho_1 + k_N)t) - 1] \, M_z^o\}}{[f^+ (1 - \zeta_{NOE}) - f^-(1 + \zeta_{NOE}) + 2\zeta_{NOE}] [\exp((\rho_1 + k_N)t) - 1] \, M_z^o} \tag{5a}$$

$$k_R = \frac{2\zeta_{ROE}(\rho_2 + k_R)M_y(0)}{[f^+(1 - \zeta_{ROE}) - f^-(1 + \zeta_{ROE})][\exp((\rho_2 + k_R)t) - 1] \, M_y^o} \tag{5b}$$

Signals for $\phi_1 = -x$ and $\phi_1 = x$ (water magnetization parallel or antiparallel to amide proton magnetization) are recorded in an interleaved manner and stored separately. During processing the signal intensities are combined to calculate ζ as described in Eq. 4 and, with the values of $(\rho_1 + k_N)$ and $(\rho_2 + k_R)$ measured as described in the Results and Discussion section, k_N and k_R rate constants are calculated from Eq. 5.

Since the NOESY mixing period, τ, is long compared to ρ_1^{-1} but short compared to the T_1 of the water, the intensity in the NOE difference spectrum asymptotically approaches a 'steady-state', $\Delta M_z(\infty) = M_z^+ (\infty) - M_z^-(\infty)$, which follows from Eq. 3a:

$$\Delta M_z(\infty) = \frac{k_N(f^+ - f^-)}{\rho_1 + k_N} M_z^o \tag{6a}$$

Similarly, the intensity of an amide correlation in the ROESY difference spectrum asymptotically approaches a 'steady-state', $\Delta M_y(\infty)$, given by:

$$\Delta M_y(\infty) = \frac{k_R(f^+ - f^-)}{\rho_2 + k_R} M_z^o \qquad (6b)$$

In conventional ROESY experiments, the mixing period typically is set to values shorter than or equal to the $T_{1\rho}$ value of the protein protons of interest. Much longer mixing times result in vanishingly weak signal intensities. In the present case, the $T_{1\rho}$ value of H_2O is much longer than the $T_{1\rho}$ values of the amide protons and a long ROESY mixing period actually results in the highest intensity in the difference spectrum. An additional benefit of the very long mixing time is that it eliminates NOEs to protons of the macromolecule that resonate in the vicinity of H_2O; these protons have a $T_{1\rho}$ value that is much shorter than the ROESY mixing time. This means that even in the absence of ^{13}C labeling, the long-mixing-time ROESY can be used to selectively observe interactions with H_2O. The use of a long mixing time in a ROESY experiment is much less problematic than in a NOESY experiment because, in contrast to NOEs, indirect ROE effects (spin diffusion) are opposite in sign relative to the direct ROE effect. As a consequence, indirect effects are partially offset by direct effects and tend to be weak (Bax et al., 1986; Bauer et al., 1990).

EXPERIMENTAL

Experiments were performed on a sample of the protein calcineurin B (2.3 mM) in the presence of the nondeuterated detergent CHAPS (25 mM) (Anglister et al., 1993a), in 95% H_2O/5% D_2O, 16 mM $CaCl_2$, pH 4.9, at 37 °C. Spectra have been recorded on a Bruker AMX 600 spectrometer, equipped with a triple resonance probehead with a self-shielded z-gradient, and an in-house built gradient pulse-shaping unit and amplifier. Each difference spectrum results from two interleaved $100^*(t_1) \times 600^*(t_2)$ datasets (where n* refers to n complex data points), with acquisition times of 75 ms (t_1) and 65 ms (t_2). The delay time between scans was 2.1 s, and the measuring times were 14.5 h for the NOE difference spectrum (Fig. 2A) and the 25-ms ROESY difference spectrum (Fig. 2B), and 6.5 h for the 100-ms ROESY difference spectrum (Fig. 2C). Data were apodized with a 60° shifted sine-bell filter in the t_1 dimension, and with a 60° shifted squared sine-bell filter in the t_2 dimension prior to zero-filling and Fourier transformation.

RESULTS AND DISCUSSION

Figure 2A shows the NOESY difference spectrum (mixing time 60 ms), i.e. the difference of the 2D HSQC spectra recorded with $\phi_1 = -x$ and $\phi_1 = x$. The ROESY difference spectra recorded for calcineurin B with 25 and 100 ms mixing times are shown in Figs. 2B and C, respectively. The latter mixing time is about seven times longer than the average $T_{1\rho}$ of the protein. As H^α protons that overlap with the water resonance have $T_{1\rho}$ values much shorter than the H_2O resonance, the long ROESY mixing time provides an additional filter for removing intraprotein ROE interactions with H^α. For $k_R \ll \rho_2$ (≈ 75 s^{-1}), the resonance intensity in the difference spectrum is expected (Eq. 2b) to be $\sim 15\%$ larger for the 100-ms mixing period (Fig. 2C) compared to the 25-ms

difference spectrum (Fig. 2B). After correcting for the numbers of transients acquired in the short- and long-mixing-time ROESY experiments, this expected increase in resonance intensity is in good agreement with the experimentally observed increase of 10–20%.

In order to calculate exchange rates from Eq. 5, reasonable estimates for ρ_2, i.e. $1/T_{1\rho}$, and the ρ_1 spin flip rate are required. An estimate for $T_{1\rho}$ is obtained from separate HSQC experiments similar to the ROESY experiment in Fig. 1B, where the selective water inversion (between points a and c) is replaced by a selective 90° pulse applied to the H_2O resonance, followed by a 10-ms gradient to dephase the water magnetization completely. Values for $T_{1\rho}$ are then determined by measuring the ^1H–^{15}N correlation intensity as a function of the duration of the spin-lock pulse in Fig. 1B. As hydrogen exchange during the spin-lock pulse also results in a loss of amide proton magnetization, this experiment yields the sum of the two rates $\rho_2 + k_R$. Values for this sum are given in Table 1. Similarly, the ρ_1 spin flip rate is estimated by measuring the decay of the $H_z^N N_z$ magnetization after the first INEPT part of the Overbodenhausen experiment (Kay et al., 1992; Peng and Wagner, 1992). To a good approximation, in the macromolecular limit this decay rate equals the sum of the proton spin flip rate ρ_1, the inverse of the ^{15}N T_1, and k_N. Using an average value of 700 ms for $T_1(^{15}N)$, values for $\rho_1 + k_N$ have been determined experimentally and are listed in Table 1.

Magnetization exchange rates have been derived from the resonance intensities in the 60-ms NOESY and the 25-ms ROESY spectra and are also presented in Table 1. The k_N and k_R values have been obtained from Eq. 5 using the $\rho_1 + k_N$ and $\rho_2 + k_R$ values determined in the manner described above and a value of 0.8 for $M_{z,y}(0)$. For most amides that show an interaction with water the k_N and k_R values are found to be very similar, indicating that these interactions are due to hydrogen exchange. Most of these rates fall into the 1–8 s^{-1} range (Table 1). However, approaching the N-terminus, the k_N and k_R values rapidly increase from 1–2 s^{-1} (Ala[5]) to 12 s^{-1} for Asn[3]. His[14] also shows very rapid k_N and k_R rates (~ 20 s^{-1}), indicating fast hydrogen exchange.

Most interesting is the relatively rapid amide hydrogen exchange observed for residues Val[84] through Lys[88]. Calcineurin B is homologous to calmodulin (CaM) and calcineurin B residues Val[84]–Lys[88] are analogous to residues Lys[77]–Ser[81] in calmodulin. In the crystal structure of calmodulin, these five residues are part of a 27-residue so-called 'central helix' (Babu et al., 1988), but in solution they are highly flexible and nonhelical (Barbato et al., 1992) with rapid amide hydrogen exchange rates (Spera et al., 1991). NOE and J coupling data indicate that in calcineurin B a nonhelical region (Phe[82]–Asp[87]) is also present between the fourth and fifth helix (Anglister et al., 1993b). The present data indicate that most residues in this nonhelical region are also subject to relatively rapid amide hydrogen exchange, similar to what was observed in calmodulin.

Exchange with solvent is also observed in the region from Asn[122] to Gln[128]. These residues are located in a loop that connects the F-helix of the third EF-hand with the E-helix of the fourth EF-hand (Anglister et al., 1993b). Rapid amide hydrogen exchange for the analogous residues in calmodulin has been reported by Spera et al. (1991).

Although for most residues k_N and k_R are identical within experimental error, for a number of amides significantly different k_N and k_R values are obtained. For example, for Ser[13] k_R is three times smaller than k_N, indicative of a competition between the effect of hydrogen exchange and ROE with either bound water or another protein proton that is in rapid exchange with water (most likely Ser[13]-O$^\gamma$H). For residues Ser[37], Glu[41], Glu[42], Ser[45], Ser[80], Ser[83], Glu[111] and Thr[136], k_R rates are of negative sign with a certainty of more than two standard deviations, indicating that
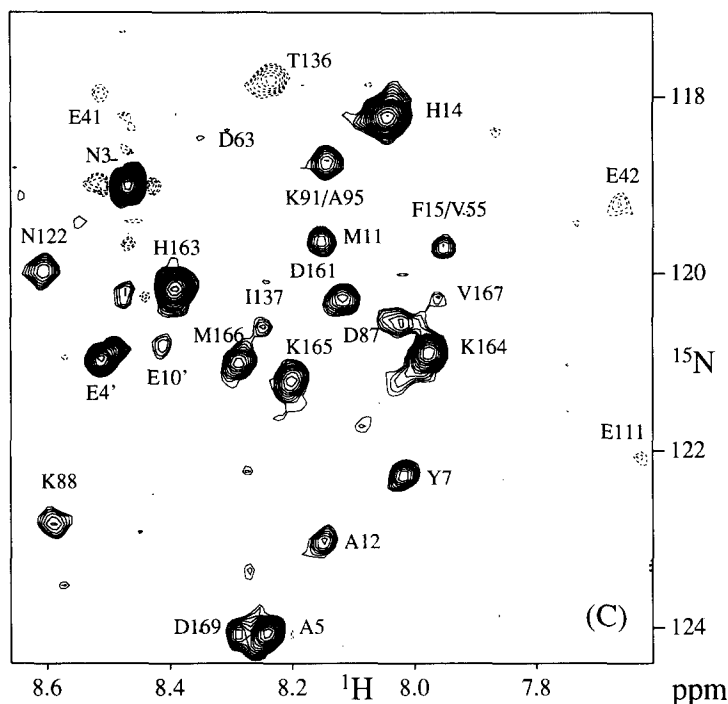
(A)

(B)
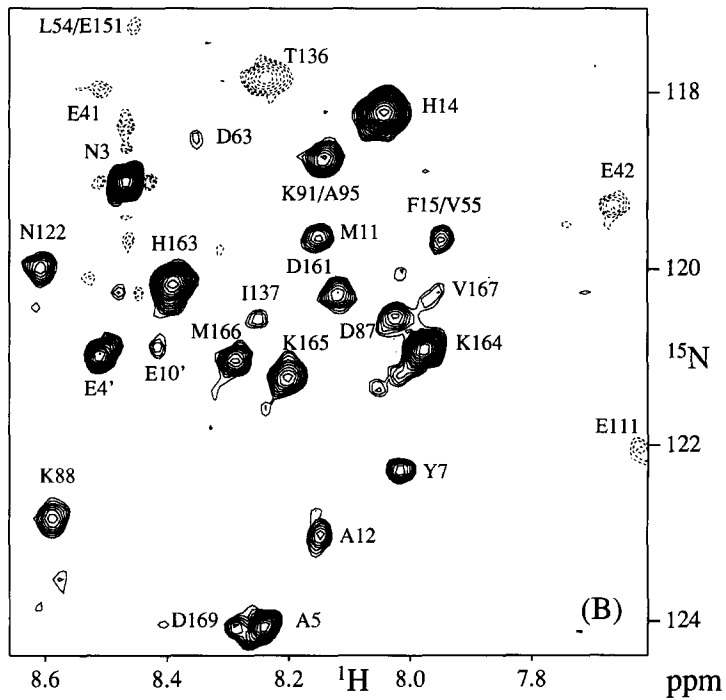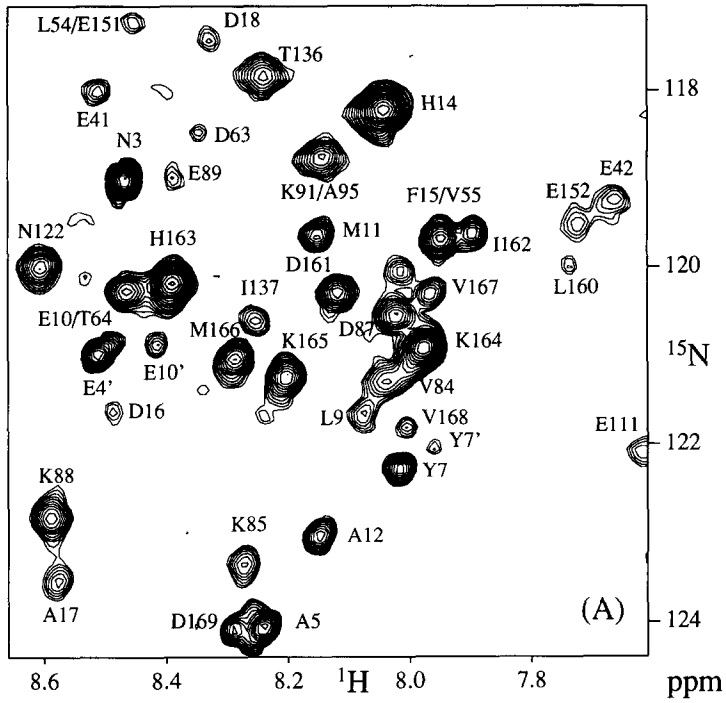
Fig. 2. Small regions of the water–protein NOE and ROE HSQC difference spectra recorded with the pulse schemes of Fig. 1 for the protein calcineurin B. (A) NOESY difference spectrum, recorded with a 60-ms mixing time (total acquisition time 14.5 h). (B,C) ROESY difference spectra, recorded with 25-ms (B) and 100-ms (C) mixing time (total acquisition times of (B) 14.5 h and (C) 6.5 h). Dashed contours indicate negative resonances. Contours are spaced by a factor of 1.25.

the magnetization exchange with water is dominated by NOE/ROE effects and not by direct exchange of the amide proton. For Glu^{42}, Ser^{80} and Thr^{136} the k_R values are very close to the theoretical limit of $-2k_N$, as expected for a pure ROE interaction in the slow-motion limit. As mentioned above, a NOE/ROE to bound water cannot easily be distinguished from a NOE/ROE to, for example, a rapidly exchanging hydroxyl proton (Otting and Wüthrich, 1989). Most likely, NOE/ROE interactions with water for the serine and threonine residues are mediated via the O^γ hydroxyl proton. For residues other than serine and threonine, precise knowledge of the protein structure is needed to exclude unambiguously the possibility of indirect effects via hydroxyl or other rapidly exchanging protons. Although no structure for calcineurin B is available yet, Glu^{42} and Glu^{111}, listed above, occupy the 12th position in the first and third EF-hand-type calcium-binding loops of calcineurin B. As pointed out by Strynadka and James (1989), X-ray crystallographic results for EF-hand-type calcium-binding loops indicate that they all are very similar in structure and that the amide proton of the residue in the 11th position is frequently hydrogen bonded to a water molecule, positioning its amide proton and that of the next residue close to the water protons. However, the crystal structure also indicates that the H^N of residue 12 is in close proximity (< 3 Å) to the Ser-O^γH of the 9th residue. It is therefore likely that the interaction for these glutamic acid residues is also caused by a relay effect via Ser-O^γH. This hypothesis is supported by the fact that Glu^{74}, which is in the 12th position of the second calcium-binding loop,

TABLE 1

FRACTIONAL NOESY AND ROESY DIFFERENCE INTENSITIES (ζ), AMIDE PROTON SPIN FLIP RATES[a] (ρ_1), ROTATING-FRAME RELAXATION RATES (ρ_2), AND AMIDE–WATER MAGNETIZATION EXCHANGE RATES (k_N AND k_R) IN CALCINEURIN B

Residue	ζ_{NOE}	ζ_{ROE}	$\rho_1 + k_N$	$\rho_2 + k_R$	k_N	k_R
N^3	0.793	0.400	14.7	25.0	11.9 (0.1)[b]	12.5 (0.5)
E^4	0.181	0.095	6.7	14.6	3.5 (0.1)	3.4 (0.1)
$E^{4'c}$	0.109	0.065	5.5	13.7	2.2 (0.0)	2.4 (0.1)
A^5	0.071	0.039	5.1	12.5	1.5 (0.0)	1.4 (0.0)
S^6	0.107	0.054	6.4	16.7	2.2 (0.0)	1.9 (0.1)
$S^{6'c}$	0.089	0.041	5.3	14.0	1.8 (0.1)	1.5 (0.3)
Y^7	0.039	0.018	6.6	21.3	0.9 (0.0)	0.6 (0.1)
$Y^{7'c}$	0.025	0.007	5.4	18.0	0.5 (0.1)	0.2 (0.2)
L^9	0.019	0.002	7.8	30.3	0.5 (0.0)	0.1 (0.1)
$E^{10'c}$	0.062	0.045	8.5	29.6	1.5 (0.2)	1.3 (0.4)
M^{11^-}	0.051	0.037	9.4	34.4	1.3 (0.1)	1.0 (0.1)
A^{12}	0.058	0.041	8.8	33.5	1.4 (0.1)	1.1 (0.1)
S^{13}	0.160	0.044	10.3	36.9	3.6 (0.1)	1.2 (0.1)
S^{13c}	0.162	0.066	8.9	27.5	3.4 (0.2)	2.0 (0.6)
H^{14}	1.480	1.418	27.5	80.0	21.8 (0.5)	19.1 (4.7)
D^{16}	0.029	−0.002	12.8	59.4	0.8 (0.2)	0.0 (0.4)
A^{17}	0.044	0.054	13.7	71.7	1.3 (0.1)	0.8 (0.3)
D^{18}	0.014	0.019	12.5	60.7	0.4 (0.1)	0.4 (0.2)
S^{37}	0.060	−0.075	13.7	65.5	1.7 (0.2)	−1.3 (0.4)
V^{40}	0.032	−0.022	19.2	97.6	1.1 (0.3)	−0.2 (0.6)
E^{41}	0.033	−0.075	15.4	78.9	1.0 (0.1)	−1.0 (0.4)
E^{42}	0.038	−0.223	20.8	95.1	1.4 (0.2)	−2.4 (0.8)
S^{45}	0.053	−0.098	13.3	61.4	1.5 (0.2)	−1.8 (0.6)
D^{65}	0.011	−0.016	11.6	59.2	0.3 (0.1)	−0.3 (0.2)
S^{80}	0.051	−0.259	16.9	72.7	1.6 (0.2)	−4.0 (0.9)
Q^{81}	0.018	−0.072	15.3	80.3	0.6 (0.2)	−1.0 (0.5)
S^{83}	0.054	−0.045	12.7	56.4	1.5 (0.1)	−0.9 (0.3)
V^{84}	0.089	0.045	13.3	60.4	2.4 (0.2)	0.8 (0.4)
K^{85}	0.057	0.025	12.7	65.0	1.6 (0.1)	0.4 (0.3)
G^{86}	0.367	0.324	18.8	68.6	8.6 (0.3)	5.3 (0.8)
D^{87}	0.096	0.077	12.9	52.0	2.5 (0.1)	1.6 (0.2)
K^{88}	0.178	0.262	17.5	71.9	4.9 (0.2)	4.1 (0.9)
E^{89}	0.020	0.023	13.8	66.8	0.6 (0.1)	0.4 (0.2)
S^{108}	0.060	−0.125	18.1	101.6	1.9 (0.4)	−1.2 (1.0)
G^{110}	0.035	−0.010	17.7	73.4	1.1 (0.2)	−0.2 (0.4)
E^{111}	0.053	−0.177	20.2	87.6	1.8 (0.3)	−2.1 (0.9)
N^{122}	0.026	0.084	14.0	62.0	0.8 (0.1)	1.5 (0.2)
N^{123}	0.032	0.021	12.7	62.6	0.9 (0.1)	0.4 (0.2)
L^{124}	0.010	0.006	10.8	59.7	0.3 (0.1)	0.1 (0.2)
K^{125}	0.016	−0.071	16.2	80.8	0.5 (0.1)	−1.0 (0.4)
D^{126}	0.299	0.384	20.6	90.4	7.9 (0.3)	4.4 (1.0)
T^{127}	0.292	0.299	18.1	67.8	7.2 (0.2)	5.0 (0.7)
Q^{128}	0.024	0.009	16.8	82.4	0.8 (0.2)	0.1 (0.4)
K^{135}	0.013	−0.000	16.2	74.6	0.4 (0.1)	0.0 (0.4)
T^{136}	0.177	−1.000	20.5	94.3	5.3 (0.3)	−10.8 (2.8)

TABLE 1 (continued)

Residue	ζ_{NOE}	ζ_{ROE}	$\rho_1 + k_N$	$\rho_2 + k_R$	k_N	k_R
D^{143}	0.010	−0.025	12.9	61.2	0.3 (0.1)	−0.5 (0.3)
S^{149}	0.065	−0.106	21.0	104.3	2.2 (0.5)	−1.0 (1.3)
E^{152}	0.062	−0.138	21.7	97.7	2.2 (0.3)	−1.4 (1.2)
G^{159}	0.038	0.035	10.6	46.5	1.0 (0.1)	0.8 (0.2)
L^{160}	0.028	0.007	12.4	51.5	0.8 (0.2)	0.1 (0.6)
D^{161}	0.083	0.054	11.1	42.3	2.1 (0.1)	1.3 (0.2)
I^{162}	0.035	−0.007	9.7	39.2	0.9 (0.1)	−0.2 (0.1)
H^{163}	0.335	0.284	15.3	50.2	7.3 (0.1)	6.2 (0.4)
K^{164}	0.308	0.239	14.1	44.1	6.7 (0.1)	5.7 (0.4)
K^{165}	0.108	0.080	9.7	34.5	2.5 (0.1)	2.2 (0.2)
M^{166}	0.094	0.071	9.3	34.1	2.2 (0.1)	2.0 (0.2)
V^{167}	0.026	0.009	7.7	29.9	0.6 (0.1)	0.3 (0.1)
V^{168}	0.010	−0.003	6.1	23.7	0.2 (0.0)	−0.1 (0.1)
D^{169}	0.027	0.014	5.4	16.7	0.6 (0.0)	0.5 (0.1)
V^{170}	0.008	−0.001	3.1	10.0	0.2 (0.0)	0.0 (0.0)

[a] All rates are given in s^{-1}.

[b] Values in brackets represent estimated errors, based on the root-mean-square level of the noise in the spectra from which the rates are derived.

[c] Residues correspond to a second conformation of the N-terminal region (Anglister et al., 1993b).

does not show an interaction with water and this loop is the only one with a non-serine residue (aspartic acid) in the 9th position. Residue Glu[152] occupies the 12th position in the fourth EF-hand and its ROE interaction with water is only barely above the signal-to-noise threshold.

Because ρ_2 is much faster than ρ_1, the ROESY difference spectrum is inherently less sensitive than the NOESY difference spectrum. For a number of backbone amide protons, the error in the ROESY intensities becomes so large that the NOE and exchange mechanisms cannot be distinguished. From the noise level of the NOESY difference spectrum and from the intensity of a typical resonance in the NOESY reference spectrum ($\phi_1 = -x$), a lower bound calculated for the detectable water exchange rate is ~ 0.2 s^{-1}, assuming a proton spin flip rate (ρ_1) of 15 s^{-1}. For intense resonances which in addition have a low ρ_1 value, such as the C-terminal residue Val[170], this lower bound is ~ 0.02 s^{-1}.

The simple and sensitive methods presented above rapidly identify amide protons that are in fast exchange with solvent, or that have a NOE interaction with bound water or with a rapidly exchanging proton. The methods can be applied to proteins uniformly enriched with ^{15}N and ^{13}C, selectively observing the interaction with water by purging all signals from protons that are attached to ^{13}C. Alternatively, the interaction with water can be studied selectively by virtue of its much longer $T_{1\rho}$ value compared to protein protons, thereby removing the necessity for ^{13}C enrichment. Simple extensions of the methodology described above, which make it applicable to the study of NOE interactions to nonlabile ^{13}C-attached protons, are presently under investigation.

638

ACKNOWLEDGEMENTS

REFERENCES

Anglister, J., Grzesiek, S., Ren, H., Klee, C.B. and Bax, A. (1993a) *J. Biomol. NMR*, **3**, 121–126.

Anglister, J., Grzesiek, S., Wang, A., Ren, H., Klee, C.B. and Bax, A. (1993b) *Biochemistry*, in press.

Babu, Y., Bugg, C.E. and Cook, W.J. (1988) *J. Mol. Biol.*, **204**, 191–204.

Barbato, G., Ikura, M., Kay, L.E., Pastor, R.W. and Bax, A. (1992) *Biochemistry*, **31**, 5269–5278.

Bauer, C.J., Frenkiel, T.A. and Lane, A.N. (1990) *J. Magn. Reson.*, **87**, 144–152.

Bax, A., Sklenar, V. and Summers, M.F. (1986) *J. Magn. Reson.*, **70**, 327–331.

Bax, A. and Pochapsky, S.S. (1992) *J. Magn. Reson.*, **99**, 638–643.

Bodenhausen, G. and Ruben, D.J. (1980) *Chem. Phys. Lett.*, **69**, 185–188.

Clore, G.M., Bax, A., Wingfield, P.T. and Gronenborn, A.M. (1990) *Biochemistry*, **29**, 5671–5676.

Englander, S.W. and Kallenbach, N.R. (1984) *Q. Rev. Biophys.*, **16**, 521–655.

Ernst, R.R., Bodenhausen, G. and Wokaun, A. (1987) *Principles of Nuclear Magnetic Resonance in One and Two Dimensions*, Clarendon Press, Oxford, p. 187.

Grzesiek, S. and Bax, A. (1993) *J. Am. Chem. Soc.*, in press.

Ikura, M. and Bax, A. (1992) *J. Am. Chem. Soc.*, **114**, 2433–2440.

Jeener, J., Meier, B.H., Bachmann, P. and Ernst, R.R. (1979) *J. Chem. Phys.*, **71**, 4546–4553.

Kay, L.E., Nicholson, L.K., Delaglio, F., Bax, A. and Torchia, D.A. (1992) *J. Magn. Reson.*, **97**, 359–375.

Kogler, H., Sørensen, O.W. and Ernst, R.R. (1983) *J. Magn. Reson.*, **55**, 157–163.

Kubinec, M.G. and Wemmer, D.E. (1992) *J. Am. Chem. Soc.*, **114**, 8739–8740.

Liepinsh, E., Otting, G. and Wüthrich, K. (1992) *Nucleic Acids Res.*, **20**, 6549–6553.

Liepinsh, E., Rink, H., Otting, G. and Wüthrich, K. (1993) *J. Biomol. NMR*, **3**, 253–257.

Marion, D., Ikura, M., Tschudin, R. and Bax, A. (1989) *J. Magn. Reson.*, **85**, 393–399.

Otting, G. and Wüthrich, K. (1989) *J. Am. Chem. Soc.*, **111**, 1871–1875.

Otting, G., Liepinsh, E., Farmer, B.T. and Wüthrich, K. (1991a) *J. Biomol. NMR*, **1**, 209–215.

Otting, G., Liepinsh, E. and Wüthrich, K. (1991b) *Science*, **254**, 974–980.

Otting, G., Liepinsh, E. and Wüthrich, K. (1991c) *J. Am. Chem. Soc.*, **113**, 4363–4364.

Peng, J.W. and Wagner, G. (1992) *J. Magn. Reson.*, **98**, 308–332.

Piotto, M., Saudek, V. and Sklenar, V. (1992) *J. Biomol. NMR*, **2**, 661–665.

Qian, Y.Q., Otting, G. and Wüthrich, K. (1993) *J. Am. Chem. Soc.*, **115**, 1189–1190.

Spera, S., Ikura, M. and Bax, A. (1991) *J. Biomol. NMR*, **1**, 155–165.

Strynadka, N.C.J. and James, M.N.G. (1989) *Annu. Rev. Biochem.*, **58**, 951–998.

Tegenfeldt, J. and Haeberlen, U. (1979) *J. Magn. Reson.*, **36**, 453–457.

Tüchsen, E. and Woodward, C. (1985) *J. Mol. Biol.*, **185**, 405–419.

Xu, R.X., Meadows, R.P. and Fesik, S.W. (1993) *Biochemistry*, **32**, 2473–2480.